ICMEs as Sources of Non-recurrent Forbush Decreases

Stephen Kahler* **and George Simnett**†

*Air Force Research Laboratory, Space Vehicles Directorate, 29 Randolph Rd, Hanscom AFB, MA 01731, USA
†School of Physics and Astronomy, University of Birmingham, B15 2TT, UK

***Abstract*. Forbush decreases (FDs) in neutron monitor (NM) counting rates are caused by enhanced magnetic fields in interplanetary shocks and solar ejecta that shield the Earth from galactic cosmic rays (GCRs). The solar origins of those ejecta can be observed as coronal mass ejections (CMEs) in coronagraphs and in heliospheric imagers such as the Solar Mass Ejection Imager (SMEI), launched into Earth orbit in January 2003. In our previous ICRC work [11] all FDs of $> 2\%$ observed with the Oulu NM through May 2005 were compared with SMEI observations to search for the white light signatures of interplanetary CMEs (ICMEs) responsible for the FDs. We now expand the FD-ICME study through the end of 2008 using updated SMEI and LASCO CME catalogs and a higher $> 3\%$ FD threshold to test our earlier result and characterize the ICMEs associated with FDs. We found an excellent association of SMEI CMEs with those FDs and for each of the associated SMEI CMEs a good associated SOHO/LASCO CME candidate was also found. The SMEI heliospheric observations provide information on the approximate spatial locations and trajectories of large ICMEs that may result in FDs and hence can be useful as a space weather tool.**

***Keywords*: Forbush Decreases, Interplanetary CMEs, Galactic Cosmic Rays**

I. Introduction

SMEI is an instrument designed to detect and forecast the arrival of interplanetary coronal mass ejections (ICMEs) and other heliospheric structures which are moving towards the Earth [24]. The instrument contains three CCD cameras, each with a field of view of $60° \times 3°$, which are mounted onto the spacecraft such that they scan most of the sky every 102-min orbit. To exclude light from the solar disk, a baffle system allows sky viewing only to within about 20° of Sun center. The sunward pointing system is offset $\sim$8.7° south of the ecliptic plane. The detectors are sensitive over the optical waveband, and the sensitivity is adequate to detect changes in sky brightness equivalent to a tenth magnitude star in one square degree of sky. To detect large ICMEs in the SMEI field of view, stellar images and the signal from the zodiacal dust cloud are subtracted from the sky images. The SMEI instrument and mission are described in [6] and [10]. SMEI was launched 6 January 2003 on the Coriolis spacecraft into a Sun-synchronous polar orbit. In the first 1.5 years of operation SMEI observed 139 ICMEs, at least 30 of which could be tracked to 1 AU and beyond and were associated with major geomagnetic storms [25] (Figure 1).

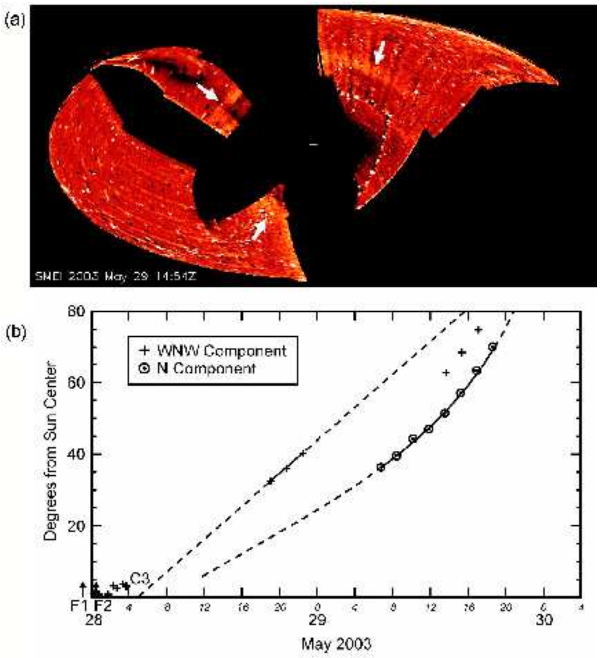

Fig. 1: [top] An Earthward-directed ICME detected by SMEI. The image format is an all-sky Aitoff projection in solar ecliptic coordinates with $1° \times 1°$ pixels and the Sun at the center. Data gaps are due to bright objects or energetic particle fluxes. The SOHO/LASCO observed two nearly simultaneous halo CMEs associated with two X-class flares, at 23:07 UT on May 27 and 00:27 UT on 28 May 2003. The SMEI ICME appeared as three contiguous arcs, shown by the white arrows. [bottom] The elongation angle versus time plot showing that the ICME components had different angular velocities. F1 and F2 indicate flare times. This is Figure 8 of [25].

Forbush Decreases (FDs) are transient decreases in the counting rates of GCRs that last typically for about a week. There are two basic types [4] of FDs. The first consist of recurrent decreases, with gradual onsets and more symmetric profiles. These are often associated with corotating interaction regions in the solar wind [18], [20] originating from long-lived coronal holes. FDs of the second type are marked by sudden onsets, reaching maximum depression in about a day, often in two stages [4], and followed by a gradual recovery [23]. In both cases it is understood that the decreases in GCR intensities result from large-scale (> 0.1 AU) increases in the interplanetary magnetic fields that modulate the scattering and convection of the GCRs [5], [26], [2]. Note that the gyroradius of a 10-GeV proton in a typical solar wind field of 10 nanotesla is 0.02 AU. GCR fluxes at 1 AU have generally been well anti-correlated with the occurrence rates of CMEs observed at the Sun [17] or at 1 AU [5]. In several specific cases [3], [15], [16] the GCR variations have been used to model the structures of ICME magnetic flux ropes.

Geomagnetic storms are also associated with ICMEs and have been the topic of many investigations, generally correlating ICME properties with the geomagnetic Dst index [27], [14], [29], [13], [21]. It would be useful to be able to forecast FDs, as we learn to use the white-light coronagraph CME and SMEI ICME observations to forecast geomagnetic storms [9], [25]. In principle, prediction of FDs should be somewhat simpler than prediction of geomagnetic storms since the former depend primarily on the magnitude of the interplanetary magnetic field enhancement while the latter depend on both the magnitude and direction of the field disturbance [19], [30]. Since we can't remotely observe the approaching interplanetary magnetic field features that lead to FDs, we want to determine how the white light observations of ICMEs may be useful for forecasting FDs. ICMEs are characterized by enhanced magnetic fields and often preceded by turbulent fields, which may cause FDs by deflections and scattering, respectively. However, enhanced pressures in ICMEs may cause super-radial expansions [7] that decrease their ambient densities and thus cause many ICMEs to become undetectable in the SMEI observations of the inner heliosphere.

In our earlier work [11] we selected FDs of >2% observed with the Oulu neutron monitor to compare with SMEI ICMEs to determine how well the SMEI observed those ICMEs that resulted in the FDs. We found SMEI ICME candidates for all 14 FDs for which SMEI observations were available and LASCO CME associations [28] for each ICME. At that time SMEI observations were complete only through late 2004. We now have SMEI observations through the end of 2008, an additional 4 years, so we can do a more comprehensive survey through the end of solar cycle 23 to explore how SMEI observations of ICMEs can be useful in predicting FDs at 1 AU.

II. Data Analysis

We used neutron monitor records from the Oulu, Finland, Cosmic Ray Station to search for FDs over the period March 2003 through the end of 2008. That station is located at a high geographic latitude of 65° and has a low cutoff rigidity of 0.78 GV. In our previous work [11] we selected as FDs all >2% decreases in counting rates for which the maximum decrease occurred within 3 days of the onset. Here we have changed the decrease threshhold to >3%, which omits only two events from our earlier work. Figure 2 shows the Oulu Neutron Monitor counting rate profile for the two FDs on 22 and 26 July 2004, with decreases of 4% and 8%, respectively.

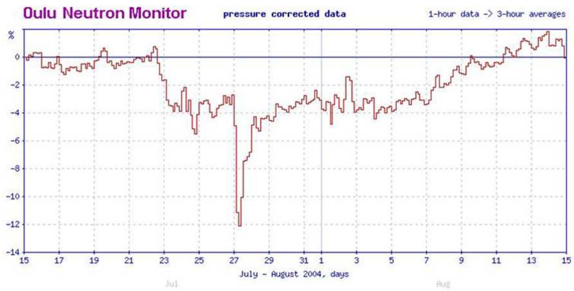

Fig. 2: The Oulu neutron monitor counting rate data showing the two non-recurrent FDs of 22 and 26 July 2004 of Table 1. From [11].

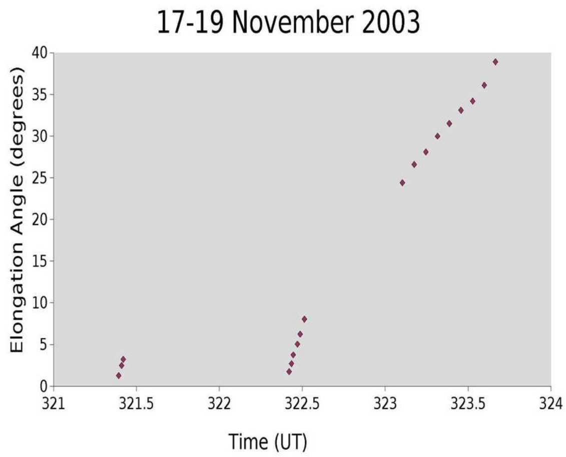

Fig. 3: Plot of the observed solar elongation angles versus time for the combined LASCO (lower points) and SMEI (upper points) candidate CMEs associated with the 20 November 2003 FD of Table I. Two LASCO CMEs are shown. The earlier CME is a partial halo with a speed of 1061 km/s; the later one is a full halo with a measured speed of 1660 km/s. The later CME on day 322 appears to be a better fit to the SMEI ICME and is listed in Table I. The SMEI CME angular speeds are determined from these plots. From [11].

Table I gives the onset dates and our estimated durations and decreases of all the non-recurrent Oulu >3% FDs through the end of 2008, followed by their estimated onset times at Earth based on times of associated increases in the IMF intensities (in italics) or, where available, their storm sudden commencements (SSCs). For each FD we list in columns 5 and 6 the date and time of first observation of a candidate associated ICME observed in SMEI. The seventh column gives ΔT, the time in hours by which the first SMEI observation of the ICME preceded the FD onset. Those are followed by the ICME azimuth angles measured in degrees counterclockwise (CCW) from solar north, and

TABLE I: Non-recurrent FDs and Associated SMEI CMEs

Onset Date	Dura. Days	Decr. %	SSC UT	SMEI Date	SMEI UT	ΔT hrs	Azimuth CCW	Speed Deg/hr	LASCO CME Day/UT,Azim.,speed	IMF B(nt)	IMF n(/cc)
2003											
08 Apr	7	3	0111	07 Apr	1640	9	071°	0.93	05/1450, 105°, 1153	16	42
29 May	5	8	1224	28 May	1653	20	284°	1.76	28/0050, halo, 1366	29	45
21 Oct	8	4	*1000*	20 Oct	0430	29	108°	0.71	18/1530, halo, 627	12	10
24 Oct	5	3	1524	24 Oct	0652	9	101°	3.37	23/0854, 053°, 1406	34	54
29 Oct	7	22	0611	28 Oct	1303	17	297°	2.57	28/1130, halo, 2459	47	DG
15 Nov	5	5	*0400*	14 Nov	0511	23	129°	1.31	13/0930, 049°, 1141	13	10
20 Nov	9	4	0803	19 Nov	0548	26	150°	2.34	18/0850, halo, 1660	55	25
2004											
06 Jan	6	5	*1700*	06 Jan	0023	17	117°	1.92	DATA GAP	17	06
22 Jan	6	7	0137	21 Jan	0348	22	133°	0.71	20/0006, halo, 965	28	20
22 Jul	5	4	1036	21 Jul	1602	19	348°	1.57	20/1331, halo, 710	18	18
26 Jul	14	8	2249	26 Jul	<1736	>5	—	—	25/1454, halo, 1333	26	03
13 Sep	14	4	2003	13 Sep	1311	7	089°	3.33	12/0036, halo, 1328	27	29
07 Nov	12	6	1052	06 Nov	0217	33	122°	2.61	06/0131, halo, 818	46	69
09 Nov	9	5	0930	08 Nov	1922	14	317°	1.68	07/1654, halo, 1759	40	24
05 Dec	8	4	0746	04 Dec	0602	26	348°	1.33	03/0026, halo, 1216	35	74
2005											
02 Jan	6	4	*2200*	02 Jan	0222	20	116°	1.46	01/0054, halo, 832	14	03
17 Jan	8	15	*1100*	16 Jan	1344	21	079°	1.39	15/0630, halo, 2049	40	DG
07 May	>7	6	1916	DATA	GAP	—	—	—	06/1728, halo, 1128	20	86
15 May	10	8	0238	DATA	GAP	—	—	—	13/1712, halo, 1689	56	37
29 May	6	4	0952	DATA	GAP	—	—	—	26/1506, halo, 586	23	18
14 Jun	4	3	1835	NONE	—	—	—	—	12/0236, 277°, 590	12	14
10 Jul	>10	3	0337	09 Jul	2123	6	338°	1.87	07/1706, halo, 683	30	40
17 Jul	4	7	0134	16 Jul	1233	13	266°	2.61	15/2108, 253°, 820	14	16
24 Aug	6	6	0613	22 Aug	1025	44	082°	0.94	22/0131, halo, 1194	60	50
11 Sep	11	11	0114	10 Sep	1306	12	119°	1.49	09/1948, halo, 2257	25	DG
2006											
09 Jul	9	3	2136	09 Jul	1527	6	270°	3.20	06/0854, halo, 911	10	20
19 Aug	7	3	1131	19 Aug	0324	8	100°	1.60	DATA GAP	20	48
08 Dec	>7	4	0435	07 Dec	0312	25	135°	—	06/2012, halo, NA	12	DG
14 Dec	5	7	1414	14 Dec	0936	5	155°	—	13/0254, halo, 1774	18	17
2007											
none											
2008											
none											

approximate angular speeds in the sky plane in degrees per hour measured on plots as shown in Figures 1 and 3. For SMEI ICMEs through July 2004 we took the data from Table 1 of [11]. Data for more recent SMEI ICMEs were taken from an updated list maintained at the Air Force Research Laboratory by D. Webb. The LASCO dates and times of first CME observations, azimuth angles measured CCW from solar north, and leading edge speeds of candidate associated CMEs are taken from the LASCO CME Catalog [28]. There were typically many LASCO CMEs over the ∼2-day periods that we searched for each FD, but those we selected clearly stood out as exceptional in their widths and speeds. Figures 1 and 3 illustrate the large angular gap between the LASCO and SMEI fields of view that make the associations challenging. The last two columns give the approximate peak intensities of the interplanetary magnetic field B in nanotesla and particle density n accompanying each FD and were taken from level 2 data of the MAG and SWEPAM experiments on the ACE spacecraft at the L1 point.

SMEI observations were available for 26 of the 29 FDs in Table I. In only one case, on 14 June 2005, did we not find a reasonable candidate ICME in the SMEI observations. We note that we are using ICMEs identified in the SMEI observations prior to and independently of our identifications of the FDs. Besides the excellent FD-ICME associations, we also ask about the lead or warning times ΔT (column 7) that the SMEI data can provide. Those times range from 5 to 44 hours, with a median value of 17 hours. The largest ΔT of 44 hours is associated with the 24 August 2005 FD and is 11 hours longer than the second largest ΔT of Table I. We regard this ICME association as the weakest or least likely in the Table. The SMEI ICME list of D. Webb describes the 22 August ICME as a very faint arc, notes that there is interference from glare, and questions the reality of the feature as an ICME. In searching for an associated LASCO CME, we found an exceptionally fast (2378 km/s) halo CME observed on 22 August at 1730 UT, which would seem the most likely CME source of the 24 August FD about 1.5 days later. That LASCO CME occurred after the initial observation of our listed SMEI candidate, so we associated with the SMEI candidate the preceding fast (1194 km/s) halo CME observed in LASCO at 0131 UT on 22 August. The unusually long lead time of 44 hours and the presence of a more likely and later halo CME argue against our association, so a better summary here is that we find 24 good SMEI associations with 26 FDs. Of the two non-associations, the 14 June 2005 FD was only 3% and was not accompanied by particularly enhanced magnetic fields or densities at ACE. On the other hand, the 24 August 2005 FD was a 6% decrease and was accompanied by very high magnetic fields and densities. We should also consider the possibility that a sufficiently large ICME may miss the Earth but still modulate GCRs when the Earth lies in its shadow.

The ICME speeds range over about a factor of $\sim$4 (0.7° to 3.3°/hr), but this might be expected from model calculations of ICME angular speeds based on the Point P and Fixed-ϕ methods [12], assuming various solar source locations. The median lead time of 17 hours for first identification of ICMEs with potential impact for FDs should apply as well for geomagnetic storms.

III. Conclusions

The good association of 24 of the 26 $>$3% FDs with ICMEs observed in SMEI shows that SMEI observations can be a useful forecast tool for FDs. The associations found here appear to preclude the possibility we raised in the Introduction that super-radial expansions of the CMEs could diminish their enhanced densities and render them invisible in SMEI.

Several points require further study. First is the question of how well the density enhancements of the SMEI ICMEs correspond to the magnetic enhancements observed at Earth and how accurately their arrival times at Earth can be predicted. Transforming the observed elongation angles, angular speeds, and angular accelerations into linear distances, speeds and accelerations of the CMEs will require a much better understanding of the ICME geometry than we have at present. We do however, now have over 300 identified SMEI events through 2008 to use for such studies.

To validate further the ICME-FD association an inverse study to determine which or how many of the Earthbound SMEI ICMEs produce FDs remains to be done. There are not yet clear criteria for deciding whether a given ICME is expected to intersect Earth since elongation angles $>$90° can be expected even if the Earth does not intercept the ICME.

Finally, in this study we generally found a prominent preceding LASCO CME to associate with the subsequent Earthbound SMEI ICME and FD. A surprising recent result [8] of comparing the SMEI observations with the LASCO CMEs is that about a quarter of SMEI ICMEs have either unlikely or no CME counterparts in the LASCO observations. Such ICMEs could begin as strong solar magnetic eruptions containing negligible excess mass and unobservable by LASCO but then sweep up enough material as they propagate through the interplanetary medium to become observable as ICMEs by SMEI. If they are intercepted by the Earth, FDs and geomagnetic storms could result.

IV. Acknowledgements

We acknowledge use of the data from the Cosmic Ray Station of the University of Oulu provided on line at http://cosmicrays.oulu.fi/#database by the Sodankyla Geophysical Observatory. The LASCO CME data were taken from the CME catalog generated and maintained at the CDAW Data Center by NASA and The Catholic University of America in cooperation with the Naval Research Laboratory. SOHO is a project of international cooperation between ESA and NASA. SMEI is a collaborative project of the U.S. Air Force Research Laboratory, the University of Birmingham, U.K., NASA, the University of California at San Diego, and Boston College. Financial support has been provided by the Air Force, the University of Birmingham, and NASA. LASCO is a collaboration between the US Naval Research Laboratory, Washington, DC, the Max Planck Institute for Aeronomy, Lindau, the Laboratoire d'Astronomie Spatiale, Marseille, and the University of Birmingham.

References

[1] Badruddin and Y. P. Singh (2003), Proc. 28th ICRC, 6, 3631.
[2] A. V. Belov, R. Butikofer et al. (2003), Proc. 28th ICRC, 6, 3581.
[3] J. W. Bieber and P. Evenson (1998), Geophys. Res. Let., 25, (15), doi: 10.1029/98GL51232, 2955.
[4] H. V. Cane (2000), Space Science Rev., 93, 55.
[5] E. W. Cliver, A. G. Ling et al. (2003), Astrophys. J., 592, 574.
[6] C. J. Eyles, G. M. Simnett et al. (2003), Solar Phys., 217, 319.
[7] J. T. Gosling (2000), Proc. 28th ICRC, Invited Papers, AIP Conf. Proc. 516 (Dingus et al. eds), 59.
[8] T. A. Howard and G. M. Simnett (2008), J. Geophys. Res., 113, A08102.
[9] T. A. Howard, D. F. Webb et al. (2006), J. Geophys. Res., 111, A04105.
[10] B. V. Jackson, A. Buffington et al. (2005), Solar Phys., 225, 177.
[11] S. W. Kahler and G. M. Simnett (2005), Proc. 29th ICRC, 2, 267.
[12] S. W. Kahler and D. F. Webb (2007), J. Geophys. Res., 112, A09103.
[13] S.-M. Kang, Y.-J. Moon et al. (2006), J. Geophys. Res., 111, A05102.
[14] R.-S. Kim, K.-S. Cho et al. (2008), Astrophys. J., 677, 1378.
[15] T. Kuwabara, K. Munakata et al. (2004), Geophys. Res. Let., 31, L19803, doi: 10.1029/2004GL020803.
[16] T. Kuwabara, J. W. Bieber et al. (2009), J. Geophys. Res., in press.
[17] A. Lara, N. Gopalswamy et al. (2005), Astrophys. J., 625, 441.
[18] I. G. Richardson (2004), Space Science Rev., 111, 267.
[19] I. G. Richardson and J. Zhang (2008), Geophys. Res. Let., 35, L06S07.
[20] A. P. Rouillard and M. Lockwood (2007), Solar Phys., 245, 191.
[21] H. Song, V. Yurchyshyn et al. (2006), Solar Phys., 238, 141.
[22] S. J. Tappin, A. Buffington et al. (2004), Geophys. Res. Let., 31, L02802, doi:10.1029/2003GL018766.
[23] I. G. Usoskin, I. Braun et al. (2008), J. Geophys. Res., 113, A07102.
[24] D. F. Webb, J. C. Johnston et al. (2002), Eos, Trans., AGU, 83, 33.
[25] D. F. Webb, D. R. Mizuno et al. (2006), J. Geophys. Res., 111, A12101.
[26] G. Wibberenz, I. G. Richardson et al. (2002), J. Geophys. Res., 107, (All), 1353, doi:10.1029/2002JA009461.
[27] C.-C. Wu and R. P. Lepping (2008), Adv. Space Res., 41, 335.
[28] S. Yashiro, N. Gopalswamy et al. (2004), J. Geophys. Res., 109, A07105.
[29] Y. I. Yermolaev and M. Y. Yermolaev (2006), Adv. Space Res., 37, 1175.
[30] J. Zhang, I. G. Richardson et al. (2008), J. Geophys. Res., 113, A00A12.